

Baryon Distribution in Relativistic Heavy-Ion Collisions

Cheuk-Yin Wong

Oak Ridge National Laboratory, Oak Ridge, Tennessee 37830

(Received 4 January 1984)

We estimate the baryon distribution in highly relativistic heavy-ion collisions in order to determine the baryon impurity of the quark-gluon plasma in the central rapidity region. In the energy range of $s^{1/2}/A \sim 30\text{--}100$ GeV per nucleon, the degree of impurity, which can be improved slightly with increasing bombarding energy, is a few percent in energy density.

PACS numbers: 25.70.Np, 12.35.Eq

Recently, there has been considerable interest in highly relativistic heavy-ion collisions.¹⁻⁶ It was suggested that the energy density in the central rapidity region may exceed the critical energy density for a phase transition from ordinary confined matter to an unconfined quark-gluon plasma.⁷ Experimental investigation of the quark-gluon plasma may provide new insight into the question of quark confinement. It may also allow one to study the evolution of the early universe. As the fraction of baryons in the early universe⁸ was about 10^{-10} , it seems desirable to design a heavy-ion collider such that when the energy density in the central rapidity region is high enough for a phase transition, there is little net baryon density there.

Recent investigations reveal that the average downward shift of the projectile baryon rapidity is quite large.⁹ It is of interest to estimate the baryon momentum distribution. We shall study the baryon distribution using a Glauber-type multiple-collision model¹⁰ in which a nucleon in one nucleus makes many inelastic collisions with nucleons in the other nucleus, the probability being given by the thickness function and the total nucleon-nucleon inelastic cross section. A nucleon may change its identity during its passage through the other nucleus, but its baryon number remains unchanged. We assume further that each baryon-baryon collision results in degradation of their energies and momenta in ac-

cordance with experimental nucleon-nucleon inelastic differential cross-section data. The momentum distribution of the resultant baryon is obtained by folding the momentum distributions of all its previous collisions. This incoherent multiple-collision model is, by itself, intuitively plausible; it can also serve as a reference model whereby coherent effects due to the formation zone,¹¹ the inside-outside cascade,¹ or the formation of the quark-gluon plasma may manifest themselves as systematic deviations. It is an extension of the model of Blankenbecler *et al.*¹² to include the effect of energy degradation. The model differs from the multichain model¹³ where the momentum distribution of the colliding baryon comes from a coherent but unknown partition of the energy among the collision chains. It also differs from a previous study¹⁴ in treatment methods and kinematic constraints.

We shall focus our attention on the longitudinal momentum distribution in terms of the Feynman scaling variable x and examine first the case of nucleon-nucleus collisions for which some data are available.^{15,16} At high energies, inelastic nucleon-nucleon collisions are the dominant mechanism for slowing down the colliding nucleons and the elastic scattering can be neglected. The momentum distribution of the incident nucleon after n inelastic collisions $D^{(n)}(x_n)$ is related to that after $n-1$ inelastic collisions $D^{(n-1)}(x_{n-1})$ by

$$D^{(n)}(x_n) = \int dx_{n-1} D^{(n-1)}(x_{n-1}) w(x_{n-1}, x_n), \quad (1)$$

where the function $w(x_{n-1}, x_n)$ is the probability distribution for finding a "leading" baryon with x_n after a baryon-baryon inelastic collision if the initial Feynman scaling variable is x_{n-1} . Experimental $pp \rightarrow pX$ data at high energies show a nearly flat¹⁵ and energy-independent¹⁷ differential cross section $d\sigma/dx$ as a function of x . Thus, the normalized distribution $w(x_{n-1}, x_n)$ can be approximated by

$$w(x_{n-1}, x_n) = \theta(x_{n-1} - x_n) \theta(x_n - x_L) / (x_{n-1} - x_L), \quad (2)$$

where x_L is the lower limit of x in accordance with energy-momentum conservation. It is approximately the value of x corresponding to the projectile baryon being stopped in the target frame or the rapidity variable y being equal to the target rapidity. Initially, the momentum distribution is $D^{(0)}(x) = \delta(x-1)$. The momen-

tum distribution of the baryon after n inelastic collisions is therefore

$$D^{(n)}(x) = \frac{1}{1-x_L} \frac{1}{(n-1)!} \left[-\ln \left(\frac{x-x_L}{1-x_L} \right) \right]^{n-1} \theta(1-x)\theta(x-x_L), \quad (3)$$

which is normalized according to $\int D^{(n)}(x) dx = 1$.

In the reaction $pA \rightarrow bX$, where A is the target nucleus with mass number A and b is a baryon, the inelastic cross section $d\sigma^{pA}/dx$ can be obtained by probability arguments. We introduce the thickness function¹⁰ for nucleon-nucleon collision as

$$T_A(b_A) = \int dz_A \rho_A(b_A, z_A), \quad (4)$$

where $\int \rho_A(\vec{r}) d^3r = 1$. The probability for the incident nucleon to make an inelastic collision with a target nucleon is given by $T_A(b)\sigma_{\text{in}}$, where σ_{in} is the nucleon-nucleon inelastic cross section and is¹⁵ 31.3 mb. The cross section $d\sigma^{pA}/dx$ is

$$\frac{d\sigma^{pA}}{dx} = \int d^2b \sum_{n=1}^A \binom{A}{n} D^{(n)}(x) [T_A(\vec{b})\sigma_{\text{in}}]^n [1 - T_A(\vec{b})\sigma_{\text{in}}]^{A-n}. \quad (5)$$

To calculate $d\sigma^{pA}/dx$ for the reaction $pA \rightarrow bX$, we take a Fermi-type nuclear density distribution with a radius parameter $r_0 = 1.25$ fm and a diffuseness $a = 0.523$ fm. Both the integrations in Eqs. (4) and (5) are carried out numerically. Experimental data¹⁶ give the cross section $E d\sigma/d^3p$ at $p_t = 0.3$ GeV/c for $pA \rightarrow pX$, but the integrated cross section $x d\sigma/dx$ for $pA \rightarrow bX$ is not available. To compare with the experimental data, we shall assume that in the range of interest, $0.3 < x < 1$, these two cross sections are related by a constant. This is a reasonable assumption as the transverse momentum distribution in the range of x is only a weak function of the mass number and x , and the mass dependence of the cross sections of $pA \rightarrow pX$ and $pA \rightarrow nX$ are the same.¹⁶ The theoretical results thus obtained give good agreement with experimental data (Fig. 1). The data for Pb may seem higher than the theoretical curve, but these data need confirmation as the shape of the cross section for the $p\text{Pb} \rightarrow pX$ reaction at 24 GeV is different.¹⁸

There, the differential cross section at $x = 0.167$ is lower than that at $x = 0.75$ by about 30%, in closer agreement with the theoretical curve. The present comparison is admittedly crude, but extensive experimental data are still lacking to warrant a discussion on corrections due to coherent effects.

We generalize the above results to the collision of a target nucleus A with a projectile nucleus with a mass number B . For highly relativistic heavy-ion collisions, the range of rapidity is large. So, in the discussion of the projectile baryon distribution, it is reasonable to neglect the collisions between projectile nucleons and the shift of the rapidities of the target nucleons. Within this approximation, all the projectile nucleons are alike and degrade in energy in the same manner. We can treat them as an ensemble of spatially correlated but independent nucleons, initially located at their local impact parameter \vec{b}_B . The projectile baryon distribution after the collision is therefore

$$\frac{dN}{dx}(x) = B \int d^2b_B T_B(\vec{b}_B) \sum_{n=0}^A \binom{A}{n} D^{(n)}(x) [T_A(\vec{b} + \vec{b}_B)\sigma_{\text{in}}]^n [1 - T_A(\vec{b} + \vec{b}_B)\sigma_{\text{in}}]^{A-n}. \quad (6)$$

We consider the projectile baryon momentum distribution for head-on collision of two equal nuclei. The target baryon distribution can be obtained by a simple reflection about the mid-rapidity axis. The distribution can be divided into a no-collision part dN_{NC}^B/dy and an inelastic part dN_{IN}^B/dy . The former corresponds to those nucleons which pass through the target without an inelastic collision and comes from the $n = 0$ term in Eq. (6). It is a sharp distribution centering around the beam rapidity. Its fraction diminishes as the mass number increases.

The inelastic part consists of projectile baryons which suffer at least one inelastic collision. It comes from the sum of the $n \geq 1$ terms in Eq. (6). We calculate dN_{IN}^B/dx and convert it to dN_{IN}^B/dy . After taking into account the Fermi motion, the results are shown in Fig. 2, where we plot the quantity $(dN_{\text{IN}}^B/dy)/\pi R_A^2$ as a function of $y - y_B$, with R_A the radius of the target nucleus and y_B the beam rapidity. This quantity gives the proper baryon density in the central rapidity region at the proper time

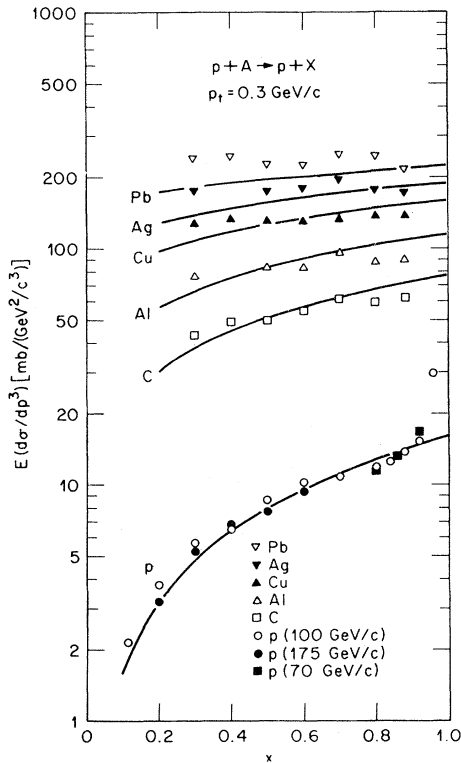


FIG. 1. Comparison of the theoretical results with the experimental data (Ref. 16) for the $pA \rightarrow pX$ reaction.

t_0 of 1 fm/c when the produced mesons and other particles begin to emerge.¹ As the mass of the colliding nuclei increases, the peak of the projectile baryon distribution becomes wider and moves to a lower rapidity. For Pb on Pb, the rapidity of the peak is shifted by ~ -2.3 . The distribution is not symmetrical about the peak. It extends well into the target rapidity region. As the bombarding energy increases, only the distributions near the target rapidity region are modified for heavy nuclei.

Of particular interest is the baryon spatial density in the central rapidity region. It has contributions from both the projectile baryons and the target baryons. For $s^{1/2}/A = 30$ GeV per nucleon, the mid-rapidity point is at $y - y_B = -4.16$. The total baryon density there at $t_0 = 1$ fm/c is 0.04 baryon/fm³ for O + O, 0.14 baryon/fm³ for Cu + Cu, and 0.28 baryon/fm³ for Pb + Pb. For the higher energy $s^{1/2}/A = 100$ GeV per nucleon, the mid-rapidity point is at $y - y_B = -5.36$. The total baryon density there at $t_0 = 1$ fm/c is 0.02 baryon/fm³ for O + O, 0.08 baryon/fm³ for Cu + Cu, and 0.21 baryon/fm³ for Pb + Pb. One can compare these densities with the energy densities ϵ of the hadrons produced in this mid-rapidity re-

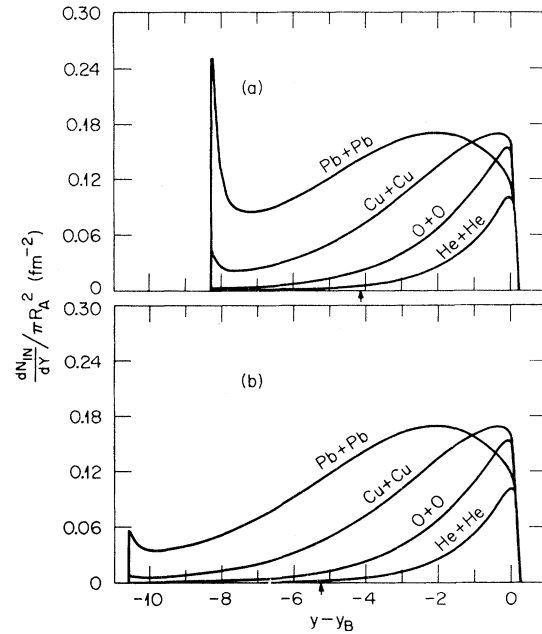


FIG. 2. The momentum distribution dN_{IN}/dy for inelastically scattered projectile baryons divided by the area πR_A^2 for head-on collisions of two equal nuclei at different energies: (a) $s^{1/2}/A = 30$ GeV per nucleon and (b) $s^{1/2}/A = 100$ GeV per nucleon. The mid-rapidity point is indicated by an arrow.

gion⁶:

$$\epsilon = 0.06A^{0.70}[0.458 \ln E + 0.354] \text{ GeV/fm}^3, \quad (7)$$

where A is the mass number of the (equal) nuclei and E is the center-of-mass energy per nucleon in gigaelectronvolts. One finds that the baryon energy density is about 6% of the total energy density for $s^{1/2}/A = 30$ GeV per nucleon, and is about 2 to 3% for $s^{1/2}/A = 100$ GeV per nucleon.

Our results indicate that in the energy range of $s^{1/2}/A \sim 30$ –100 GeV per nucleon, the baryon impurity in the mid-rapidity region is a few percent in energy density. A quark-gluon plasma with this amount of baryon impurity can still be of interest, and may allow a closer extrapolation to quark-gluon plasma of even smaller baryon fractions for astrophysical studies.

The author wishes to thank Professor W. Busza and Professor A. S. Goldhaber for helpful discussions. This research was supported by the U. S. Department of Energy under Contract No. W-7405-eng-26 with the Union Carbide Corporation.

¹J. D. Bjorken, Phys. Rev. D **27**, 140 (1983).

²K. Kajantie and L. McLerran, Phys. Lett. **119B**, 203

(1982).

³T. D. Lee, Columbia University Report No. CU-TP-226, 1981 (unpublished).

⁴M. Gyulassy, Lawrence Berkeley Report No. LBL-15175, 1982 (unpublished).

⁵J. Rafelski and M. Danos, NBS Report No. NBSIR 83-2725, 1983 (unpublished).

⁶C. Y. Wong, to be published.

⁷For example, L. McLerran and B. Svetitsky, Phys. Lett. **96B**, 195 (1981), and Phys. Rev. D **24**, 450 (1981); I. Montvay and H. Pietarinen, Phys. Lett. **115B**, 151 (1982); J. Kogut *et al.*, Phys. Rev. Lett. **48**, 1140 (1982).

⁸D. Schramm, in Proceedings of the Third International Conference on Ultra-Relativistic Nucleus-Nucleus Collisions, Brookhaven National Laboratory, September 1983 (to be published), Fermilab Report No. Conf-83/92-AST.

⁹W. Busza and A. S. Goldhaber, in Proceedings of the Third International Conference on Ultra-Relativistic Nucleus-Nucleus Collisions, Brookhaven National La-

boratory, September 1983 (to be published), Institute of Theoretical Physics Report No. ITP-SB-82, 1983.

¹⁰R. J. Glauber, in *Lectures in Theoretical Physics*, edited by W. E. Brittin and L. G. Dunham (Interscience, New York, 1959), Vol. 1, p. 315.

¹¹S. J. Brodsky, Stanford Linear Accelerator Center Report No. SLAC-PUB-3219, 1983 (unpublished); L. Landau and I. Pomeranchuk, Dokl. Akad. Nauk SSSR **92**, 535 (1953).

¹²R. Blankenbecler, A. Capella, J. Tran Thanh Van, C. Pajares, and A. V. Ramallo, Phys. Lett. **107B**, 106 (1981).

¹³A. Capella and A. Krzywicki, Phys. Lett. **67B**, 84 (1977); K. Kinoshita, A. Minaka, and H. Sumiyoshi, Prog. Theor. Phys. **61**, 165 (1979), and **63**, 928 (1980).

¹⁴J. Kapusta, Phys. Rev. C **27**, 2037 (1983).

¹⁵A. E. Brenner *et al.*, Phys. Rev. D **26**, 1497 (1982).

¹⁶D. S. Barton *et al.*, Phys. Rev. D **27**, 2580 (1983).

¹⁷F. E. Taylor *et al.*, Phys. Rev. D **14**, 1217 (1976).

¹⁸T. Eichten *et al.*, Nucl. Phys. **B44**, 333 (1972).